the following results. Anal. Calcd for $C_{11}H_{24}N_4O_4P_2Pt$: C, 24.77; H, 4.53; N, 10.50. Found: C, 23.91; H, 4.36; N, 9.69. Inspection by microscope showed the crystal surfaces coated with small spots of an amorphous black material, likely platinum. ^1H NMR in DMSO-d_6: cytosine resonances, 7.22 (d, J_{H-H} = 7.0 Hz, H_6), 6.97 (broad singlet, NH), 5.84 (d, J_{H-H} = 7.0 Hz, H_5), 3.14 (s, CH_3); phosphine resonances, 1.75 (d, $^2J_{P-H}$ = 10.9 Hz, $^3J_{Pt-H}$ = 35.6 Hz), 1.48 (d, $^2J_{P-H}$ = 10.5, $^3J_{Pt-H}$ = 30.5 Hz).

Crystallography of *cis*-$[(PMe_3)_2Pt(\mu\text{-}OH)]_2(NO_3)_2$ and *cis*-$[(PMe_3)_2Pt(\mu\text{-}1\text{-}MeCy(-H))]_2(NO_3)_2$. Transparent, colorless crystals of the μ-hydroxo complex were grown by slow evaporation of a water solution. Details of the crystal data, measurement of intensities, and data processing are summarized in Table II. The intensity data were collected on a Philips PW1100 four-circle diffractometer. Empirical absorption correction, based on ψ scans of three reflections at $\chi \approx 90°$, was applied. The structure was solved by the heavy-atom method and was refined by full-matrix procedures, anisotropically only for Pt, P(1), P(2), and O(1) atoms. No direct determination of the positions of the hydrogen atoms was attempted because of the presence of the heavy Pt atom. The programs used were those of the SHELX package.[22] Fractional coordinates and thermal parameters are given in Table A of the supplementary material. Additional details, including nonessential bond distances and angles, are available as supplementary material. The same apparatus was used for the X-ray analysis of *cis*-$[(PMe_3)_2Pt(\mu\text{-}1\text{-}MeCy(-H))]_2(NO_3)_2$ (**1**). Characteristics of the data collection processing and refinement are given in Table IV. The structure was solved by the heavy-atom method and refined by full-matrix procedures, anisotropically for all non-hydrogen atoms of the dication and isotropically for the nitrate group atoms. Bond distances and angles are listed in Tables V and VI, respectively.

Fractional coordinates and thermal parameters are reported in Table B of the supplementary material. A table of least-square planes with deviations of the relevant atoms and dihedral angles of **1** is reported as supplementary material (Table C).

(22) Sheldrick, G. M. SHELX76, Programs for Crystal Structure Determination. University of Cambridge, Cambridge, England, 1976.

Acknowledgment. Parke-Davis is gratefully acknowledged for a research grant to G.T. We thank Progetto Finalizzato Chimica Fine II, CNR, for partial financial support.

Supplementary Material Available: Tables A–C, listing fractional coordinates and thermal parameters for the two complexes and least-squares planes, deviations of relevant atoms, and dihedral angles for **1** (4 pages); Tables D and E, listing observed and calculated structure factors for both compounds (25 pages). Ordering information is given on any current masthead page.

Contribution from the Department of Medicinal Chemistry, Hiroshima University School of Medicine, Kasumi 1-2-3, Minami-ku, Hiroshima 734, Japan, Coordination Chemistry Laboratories, Institute for Molecular Science, Myodaiji, Okazaki 444, Japan, and Physics Laboratory, Faculty of Pharmaceutical Science, Teikyo University, Kaga, Itabashi-ku, Tokyo 113, Japan

Acid Properties of Zinc(II) and Cadmium(II) in Complexation with Macrocyclic Oxo Polyamine Ligands

Eiichi Kimura,*[†,‡] Tohru Koike,[†] Takeshi Shiota,[†] and Yoichi Iitaka[§]

Received February 14, 1990

The pH-metric titration study of the interaction of Zn^{II} and Cd^{II} ion with dissociable (acidic) hydrogen-containing macrocyclic polyamines **3–10** has served to distinguish inherent acid and coordination properties of these two metal ions. In complexation with monooxocyclam **3** below pH 8, Zn^{II} ion can replace the amide hydrogen and forms a planar 1:1 monooxocyclam complex $[ZnH_{-1}L]^+$ (**14**) containing the hitherto unknown deprotonated amide N^-–Zn^{II} coordination, while Cd^{II} ion does not yield such a complex. A square-pyramidal N_5Zn^{II} complex $[ZnH_{-1}L]^+$ (**16**) is formed with a pyridyl-pendant monooxocyclam **5** at pH <8, as confirmed by an X-ray structure analysis. In contrast, the larger and less acidic Cd^{II} displaces the amide proton of the same ligand to yield $[CdH_{-1}L]^+$ (**18**) at pH >10. The intermediate complex **17** containing a Cd^{II}–O(amide) bond was isolated and characterized by an X-ray structure analysis. A larger sized 16-membered macrocyclic monooxopentaamine, **10**, initially (pH <6) binds more strongly with Cd^{II} than with Zn^{II} using the four secondary nitrogen donors to form $[ML]^{2+}$, **26** and **28**. At higher pH, however, the more acidic Zn^{II} yields a more stable 5-coordinate amide-deprotonated complex, $[ZnH_{-1}L]^+$ (**27**), than the less acidic Cd^{II} does, $[CdH_{-1}L]^+$ (**29**).

Introduction

Recently, the acidic properties of zinc(II) have attracted much attention, as increasing numbers of hydrolytic enzymes (e.g. carboxypeptidases, carbonic anhydrase) are found to contain Zn^{II} in their active centers.[1,2] Unfortunately, the studies to pinpoint the inherent acid properties of the Zn^{II} ion to help understand the specific role of the Zn^{II} ion in those natural complexes are surprisingly limited, due to the following difficulties: (i) Zn^{II}, being a d^{10} metal ion, has few observable chemical properties indicating its environment and activity (i.e. the lack of UV–visible absorptions, magnetic susceptibility).[3] Sometimes, in order to circumvent these drawbacks, Ni^{II}, Co^{II}, Mn^{II}, or isotopic Cd^{II} have been substituted to pursue the action of Zn^{II} in enzymes.[4] (ii) Zn^{II} complexes are usually labile with artificial simple ligands,[5,6] thereby preventing construction of well-defined reactive site in the complicated Zn^{II}–enzyme. (iii) There have been few appropriate ligands available that allow one to focus on the microscopic role of Zn^{II}. Most often, previously designed biomimetic ligands[7,8] worked indiscriminantly with other metal ions, and few comprehensive explanations[9] were provided regarding why the active metal ion ought to be Zn^{II}, but not the other metal ions (e.g. Cu^{II}, Ni^{II}).

It was found that a tridentate, macrocyclic triamine yields a very stable and structurally well-defined Zn^{II} complex **1**,[10–13] which

† Hiroshima University School of Medicine.
‡ Institute for Molecular Science.
§ Teikyo University.

(1) Bertini, I.; Luchinat, C.; Maret, W.; Zeppezauer, M. *Zinc Enzymes*; Birkhäuser: Boston, MA, 1986.
(2) Vallee, B. L.; Galdes, A. *Advances in Enzymology*; Wiley: New York, 1984; Vol. 56, p 283.
(3) Cotton, F. A.; Wilkinson, G. *Advanced Inorganic Chemistry*, Wiley: New York, 1980.
(4) Rohm, K. H. In ref 1, Chapter 18. Sen, A. C.; Tu, C. K.; Thomas, H.; Wynns, G. C.; Silverman, D. N. In ref 24, Chapter 24. Bertini, I.; Dei, A.; Luchinat, C.; Monnanni, R. In ref 1, Chapter 27.
(5) Dakternikes, D. *Coord. Chem. Rev.* **1987**, *78*, 125–146. Dakternikes, D. *Coord. Chem. Rev.* **1985**, *62*, 1–35. Constable, E. C. *Coord. Chem. Rev.* **1982**, *45*, 329–366.
(6) (a) Kodama, M.; Kimura, E. *J. Chem. Soc., Dalton Trans.* **1978**, 1081–1085. (b) Kodama, M.; Kimura, E. *J. Am. Chem. Soc., Dalton Trans.* **1977**, 2269–2276.
(7) Woolley, P. *Nature* **1975**, *258*, 677–682.
(8) Groves, J. T.; Chambers, R. R., Jr. *J. Am. Chem. Soc.* **1984**, *106*, 630–638.
(9) Ochiai, E. *J. Chem. Educ.* **1988**, *65*, 933–946.
(10) Zompa, L. J. *Inorg. Chem.* **1978**, *17*, 2531–2536.

0020-1669/90/1329-4621$02.50/0

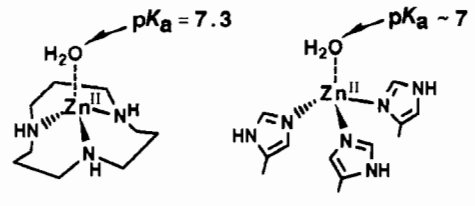

1 2

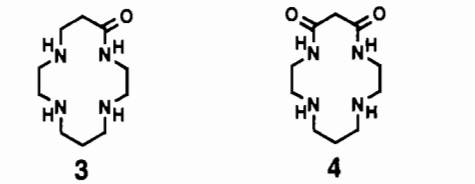

3 4

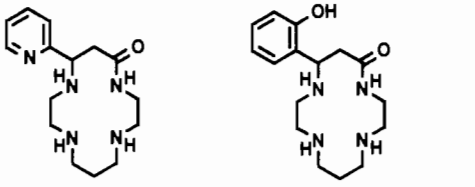

5 6

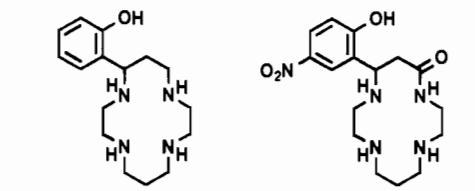

7 8

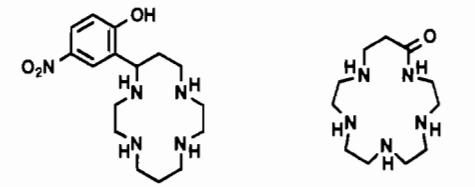

9 10

appeared to offer a good system for mimicking the active sites of Zn^{II} enzymes such as carbonic anhydrase 2.[12] In this enzyme, the Zn^{II} ion is bound with *three* imidazole donors and the fourth coordinated H_2O dissociates a proton at physiological pH, with the resulting $Zn-OH^-$ moiety playing a critical role in their catalytic actions.[14] Indeed, we have discovered that the Zn^{II} complex **1**, by forming a $Zn-OH^-$ species at physiological pH (its pK_a of 7.3 (at 25 °C) is nearly the same pK_a (ca. 7.5) of **2**), catalyzes ester hydrolysis and aldehyde hydration reactions like carbonic anhydrase,[15,16] which was reported separately.[12b] During investigation of the acidic properties of the Zn^{II}-bound H_2O in **1**, it occurred to us that potentially 3–5 coordinate ligands, such as the macrocyclic polyamines **3**–**10**,[17–25] which all contain dissociable, acidic hydrogen(s), might work as suitable ligands to help specify the acidic nature of the Zn^{II} ion in amine complexes. Since the Zn^{II} ion (d^{10}) has no specially distorted or directional ligand field, use of those ligands, even though equipped with donors from various directions, would pose little disadvantage.

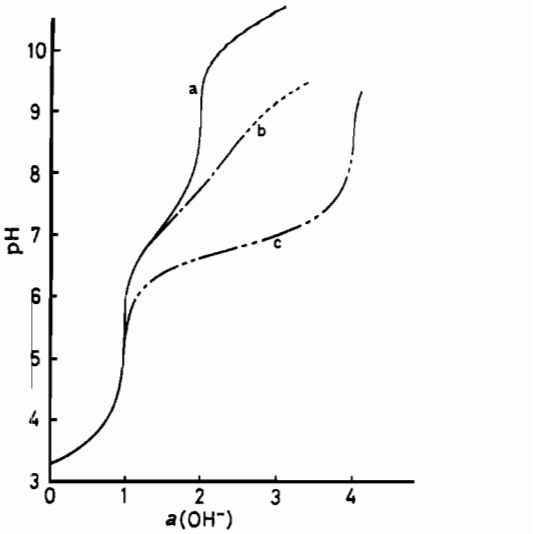

Figure 1. Titration curves for monooxocyclam **3**: (a) 1 mM of $[3 \cdot 3H^+]^{3+}$; (b) solution a + 1 mM of $CdSO_4$; (c) solution a + 1 mM of $ZnSO_4$. The dotted line indicates precipitation of cadmium(II) hydroxide.

Scheme I

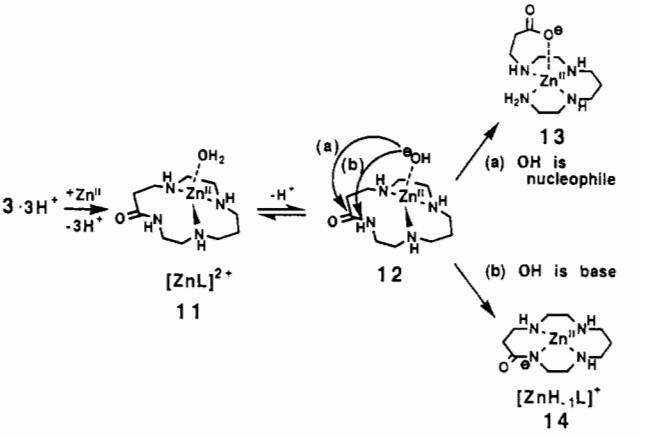

A typical example is given by monooxocyclam **3**.[17] When Zn^{II} initially binds with three NH's, it will leave an open fourth site leading to **11** or **12** (Scheme I), which then may act as a nucleophile for the amide hydrolysis to **13** or act as a base to yield **14**. By using Cd^{II} ion in place of the Zn^{II} ion, we hoped to study the inherent chemical properties that distinguish the Zn^{II} ion from the Cd^{II} ion. The complexation of the macrocyclic monooxotetraamine ligand **3** with M^{II} ions could then be compared with those of the dioxotetraamine ligand **4**,[18] pyridyl-pendant attached monooxocyclam **5**,[19,20] phenol-pendant attached 14-membered

(11) Kimura, E.; Yamaoka, M.; Morioka, M.; Koike, T. *Inorg. Chem.* **1986**, *25*, 3883–3886.
(12) (a) Kimura, E.; Koike, T.; Toriumi, K. *Inorg. Chem.* **1988**, *27*, 3687–3688. (b) Kimura, E.; Shiota, T.; Koike, T.; Shiro, M.; Kodama, M. *J. Am. Chem. Soc.* **1990**, *112*, 5805–5811.
(13) Schaber, P. M.; Fettinger, J. C.; Churchill, M. R.; Nalewajek, D.; Fries, K. *Inorg. Chem.* **1988**, *27*, 1641–1646.
(14) Silverman, D. N.; Lindskog, S. *Acc. Chem. Res.* **1988**, *21*, 30–36. Merz, K. M.; Hoffmann, R.; Dewar, M. J. S. *J. Am. Chem. Soc.* **1989**, *111*, 5636–5649. Coleman, J. E. In ref 1, Chapter 4.
(15) Pocker, Y.; Stone, T. *Biochemistry* **1967**, *6*, 668–678.
(16) Pocker, Y.; Meany, J. E. *Biochemistry* **1965**, *4*, 2535–2541.
(17) Kimura, E.; Koike, T.; Machida, R.; Nagai, R.; Kodama, M. *Inorg. Chem.* **1984**, *23*, 4181–4188.
(18) Kodama, M.; Kimura, E. *J. Chem. Soc., Dalton Trans.* **1979**, 325–329.
(19) Kimura, E.; Koike, T.; Nada, H.; Iitaka, Y. *J. Chem. Soc., Chem. Commun.* **1986**, 1322–1323.
(20) Kimura, E.; Koike, T.; Nada, H.; Iitaka, Y. *Inorg. Chem.* **1988**, *27*, 1036–1040.
(21) Kimura, E.; Koike, T.; Takahashi, M. *J. Chem. Soc., Chem. Commun.* **1985**, 385–386. Iitaka, Y.; Koike, T.; Kimura, E. *Inorg. Chem.* **1986**, *25*, 402–404.
(22) Kimura, E.; Koike, T.; Uenishi, K.; Hediger, M.; Kuramoto, M.; Joko, S.; Arai, Y.; Kodama, M.; Iitaka, Y. *Inorg. Chem.* **1987**, *26*, 2975–2987.
(23) Kimura, E.; Machida, R.; Kodama, M. *J. Am. Chem. Soc.* **1984**, *106*, 5497–5505.
(24) Kimura, E. *Pure Appl. Chem.* **1986**, *58*, 1461–1466.
(25) Kimura, E. *J. Coord. Chem.* **1986**, *25*, 1–28.

Table I. Protonation Constants (log K_n) and Zn^{II} and Cd^{II} Complex Formation Constants (log K) for Monoamide-Containing Macrocyclic Polyamines **3**, **5**, **6**, **8** and **10** at 25 °C and I = 0.1 ($NaClO_4$)[a]

	3	**5**	**6**	**8**	**10**
log K_1	10.62 ± 0.03	10.76 ± 0.03	11.09 ● 0.03	10.86 ± 0.03	9.99 ± 0.03
log K_2	7.16 ± 0.02	6.29 ± 0.02	9.63 ± 0.03	7.20 ± 0.02	9.03 ± 0.02
log K_3	3.15 ± 0.05	3.78 ± 0.03	6.40 ± 0.02	5.80 ± 0.02	5.96 ± 0.02
log K_4	*e*	<2	2.7 ± 0.2	2.5 ± 0.2	2.5 ± 0.2
log $K(ZnL)$[b]	*e*	8.60 ± 0.03	*e*	*e*	10.7 ± 0.1
log $K(ZnH_{-1}L)$[c]	0.59 ± 0.03	1.28 ± 0.03	−0.4 ± 0.1	−1.7 ± 0.1	2.3 ± 0.1
log $K(ZnH_{-2}L)$[d]	*e*	*e*	−9.6 ± 0.1	−10.1 ± 0.1	*e*
log $K(CdL)$[b]	*e*	7.15 ± 0.05	*e*	*e*	11.6 ± 0.1
log $K(CdH_{-1}L)$[c]	*e*	−3.47 ± 0.05	*e*	*e*	1.1 ± 0.1

[a] The first protonation constants (K_1) for **6** and **8** are $[L]/[H_{-1}L^-]a_{H^+}$. For the other ligands, K_1's are $[LH^+]/[L]a_{H^+}$. [b] $K(ML) = [M^{II}L]/[M^{II}][L]$ (M^{-1}). [c] $K(MH_{-1}L) = [M^{II}H_{-1}L]a_{H^+}/[M^{II}][L]$. [d] $K(MH_{-2}L) = [M^{II}H_{-2}L](a_{H^+})^2/[M^{II}][L]$ (M). [e] Negligible species under the experimental conditions.

macrocyclic tetraamines **6**–**9**,[21,22] and the larger-sized macrocyclic monooxopentaamine **10**,[23] which have all been originally synthesized and explored in our laboratory. Indeed, with these macrocyclic polyamines, we could uncover the unique nature of the Zn^{II} ion, which may be relevant to the secret of the Zn^{II} ion in the natural enzymes. Moreover, using these macrocyclic ligands, we could easily distinguish the Zn^{II} ion from the Cd^{II} ion, a fact that industrially and environmentally is very important and yet has seen limited success.[26,27]

Experimental Section

General Methods. All the starting materials were obtained commercially and were used without further purification. FT-IR spectra were obtained with a Shimazu FTIR-4200. ^1H NMR (400 MHz) spectra were recorded on a JEOL GX-400 NMR spectrometer at 25 °C. UV absorption spectra (±1 nm) were obtained with a Hitachi U-3200 spectrophotometer at 25 °C. The synthesis of dissociable H-containing ligands 3–10 were described earlier in detail.[17–25]

Potentiometric Titration. The preparation of the test solutions and the calibration of the electrode system were described earlier.[22] The ligand protonation constants are listed in Table I. The calculation methods for the Zn^{II} and Cd^{II} complex formation constants (K) are the same as those for the pyridylmonooxocyclam (**5**) Ni^{II} complex[20] and for the monooxo-[16]aneN_5 (**9**) Ni^{II} complex.[23] The temperature was maintained at 25.0 ± 0.1 °C, and the ionic strength (I) was adjusted to 0.10 M with $NaClO_4$. The titration curves are shown in Figures 1, 2, 5, and 7. The ligand protonation constants (log K_n) and M^{II} complex formation constants (log K) are given in Table I.

Preparation of the Monooxocyclam Zn^{II} Complex (14)ClO_4·2H_2O. 5-Oxo-1,4,8,11-tetraazacyclotetradecane (monooxocyclam, **3**) (210 mg, 1 mmol) and $Zn(ClO_4)_2$·6H_2O (370 mg, 1 mmol) were dissolved in 5 mL of 1 M $NaClO_4$ aqueous solution at ca. 40 °C, and the mixture was adjusted to pH 8 with 1 M NaOH. The resulting solution was filtered, and the filtrate was allowed to stand for 5 days at room temperature. Colorless needles of **14** were obtained as the monoperchlorate salt in ca. 70% yield. IR (in D_2O, cm^{-1}): 1565 (s, CO), 1100 (br, ClO_4^-). ^1H NMR (D_2O (pD 8), DSS reference): δ 1.6–1.8 (1 H, m, C–CH–C), 1.8–2.0 (2 H, m, C–CH–C, C–CH–CO), 2.3–3.3 (15 H, m, C–CH–CO, N–CH_2–C). Anal. Calcd for $C_{10}H_{21}N_4OZnClO_4$·2H_2O: C, 29.00; H, 6.08; N, 13.53. Found: C, 28.71; H, 6.20; N, 13.18.

Preparation of the Pyridylmonooxocyclam Zn^{II} Complex (16)ClO_4·3H_2O. 7-(2-Pyridyl)-5-oxo-1,4,8,11-tetraazacyclotetradecane (pyridylmonooxocyclam, **5**) (87 mg, 0.3 mmol) and $Zn(ClO_4)_2$·6H_2O (110 mg, 0.3 mmol) were dissolved in 2 mL of a 0.1 M $NaClO_4$ aqueous solution at ca. 40 °C, and the mixture was adjusted to pH 9.5 with 3 mL of a 0.1 M NaOH solution. The resulting solution was filtered, and the filtrate was allowed to stand for 2 days at room temperature. Colorless crystals of **16** were obtained as the monoperchlorate salt ((**16**)ClO_4·3H_2O) in ca. 50% yield. A crystal in a capillary was used for X-ray data collection at room temperature. IR (KBr pellet, cm^{-1}): 3440 (br OH), 3256 (NH), 2926 (CH), 2872 (CH), 1570 (s, CO), 1445, 1402, 1318, 1096 (br, ClO_4^-), 1022, 959, 930, 781, 758, 715, 625, 546. ^1H NMR (D_2O (pD 8.5), DSS reference): δ 8.53 [1 H, d, J = 4.9 Hz, HC(18)], 7.98 [1 H, m, HC(20)], 7.57 [1 H, d, J = 7.9 Hz, HC(21)], 7.48 [1 H, d–d–d, J = 7.6, 5.2, and 0.9 Hz, HC(19)], 4.56 [1 H, d–d, J = 4.3 and 3.4 Hz, HC(7)], 3.35–2.50 (13 H, m, N–CH_2–C, C–CH–CO), 2.13–1.74 (3 H, m, C–CH_2C, C–CH–CO). ^{13}C NMR (D_2O (pD 8.5), DSS reference): δ 174.6, 159.0, 149.3, 142.7, 127.6, 126.9, 60.6, 53.32, 53.29, 51.6, 50.7, 46.2, 45.1, 44.5, 31.1. One H_2O molecule in this crystal is easily removed at room temperature and 1 mmHg pressure (as judged by a gradual color change to white). Anal. (for this white solid) Calcd for $C_{15}H_{24}N_5OZnClO_4$·2H_2O: C, 36.67; H, 5.75; N, 14.26. Found: C, 36.37; H, 5.70; N, 14.19.

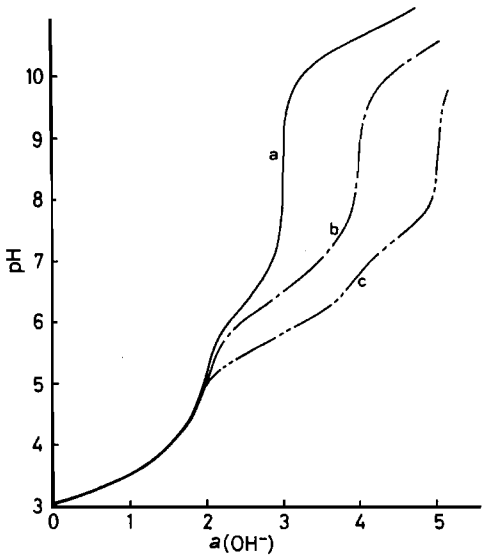

Figure 2. Titration curves for pyridylmonooxocyclam **5**: (a) 1 mM of [**5**·4H^+]$^{4+}$; (b) solution a + 1 mM of $CdSO_4$, (c) solution a + 1 mM of $ZnSO_4$.

Preparation of the Pyridylmonooxocyclam Cd^{II} Complex (17)$(ClO_4)_2$·H_2O. The pyridylmonoooxocyclam **5** (290 mg, 1 mmol) and $CdSO_4$·H_2O (226 mg, 1 mmol) were dissolved in 5 mL of 1 M $NaClO_4$ aqueous solution at room temperature and pH 9. The resulting solution was filtered, and the filtrate was allowed to stand for 1 day in a drybox. Colorless crystals of **17** were obtained as the diperchlorate salt ((**17**)-$(ClO_4)_2$·H_2O) in ca. 70% yield. IR (KBr pellet, cm^{-1}): 3440 (br, OH), 3263 (NH), 3225 (NH), 2928 (CH), 2880 (CH), 1609 (s, CO), 1560, 1439, 1368, 1304, 1285, 1144, 1117 (br, ClO_4^-) 1088, 1019, 960, 936, 774, 637, 627, 540. ^1H NMR (D_2O (pD 8.5), DSS reference): δ 8.59 [1 H, d, J = 4.8 Hz, HC(18)], 8.07, [1 H, t, J = 7.7 Hz, HC(20)], 7.60 [2 H, m, HC(19) HC(21)], 4.65 [1 H, d, J = 6.2 Hz, HC(7)], 3.8 (1 H, m), 3.3 (1 H, m), 3.3–2.8 (10 H, m), 2.7 (2 H, m), 2.2 (1 H, m), 2.0 (1 H, m), 1.7 (1 H, m). ^{13}C NMR (D_2O (pD 8.5), DSS reference): δ 176.9, 159.1, 151.0, 143.7, 128.5, 127.8, 56.7, 55.4, 55.2, 53.7, 48.9, 47.8, 44.8, 41.3, 24.7. Anal. Calcd for $C_{15}H_{25}N_5OCd(ClO_4)_2$·$H_2O$: C, 29.02; H, 4.38; N, 11.28. Found: C, 29.02; H, 4.23; N, 11.29.

Crystallographic Study. The lattice parameters and intensity data were measured on a Philips PW-1100 automatic four-circle diffractometer by using graphite-monochromated Cu Kα radiation. The structures of Zn^{II} complex **16** and Cd^{II} complex **17** were solved by the heavy-atom method and refined by the block-diagonal-matrix least-squares method. The hydrogen atoms were located on the difference electron density map and their positions were at first regularized by the standard bond lengths and bond angles and then included in the least-squares refinement with isotropic temperature factors. The final R values for **16** and **17** are 0.063 and 0.047, respectively.

(26) Alcock, N. W.; Moore, P.; Omar, H. A.; Reader, C. J. *J. Chem. Soc., Dalton Trans.* **1987**, 2643–2648.
(27) Adam, K. A.; Dancey, K. P.; Leong, A. J.; Lindoy, L. F.; McCool, B. J.; McPartlin, M.; Tasker, P. A. *J. Am. Chem. Soc.* **1988**, *110*, 8471–8477 and references therein.

Scheme II

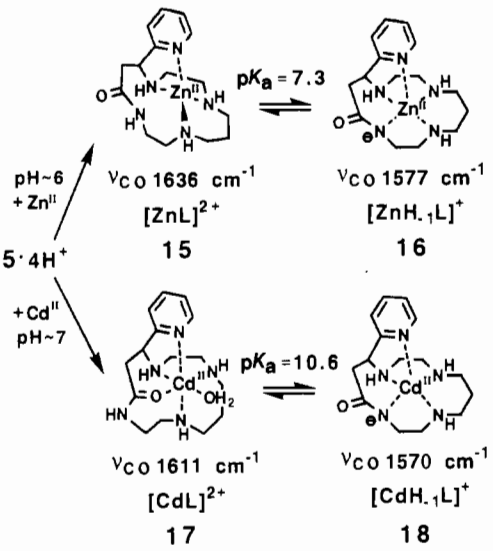

Results and Discussion

Monooxocyclam 3 Complexes with Zn^{II} and Cd^{II}. The interaction equilibrium was determined by 0.1 M NaOH titration of 1 mM of $3\cdot3H^+$ in the presence of 1 equiv of $ZnSO_4$ and $CdSO_4$ (Figure 1c,b). The smooth buffer curve for Zn^{II} (Figure 1c) does not break until four protons are neutralized at $a = 4$, implying that the Zn^{II}–**3** complexation does not halt at the stage of **11**, but goes further to neutralization of one more proton. The candidates for the resulting complex are **12**, **13**, and **14**. The supporting evidence for the amide deprotonated $[ZnH_{-1}L]^+$ (**14**) comes from the CO stretching frequency change in D_2O from 1624 cm^{-1} of the free ligand **3** to 1565 cm^{-1} assignable to the deprotonated amide group at pD 8. More concrete evidence for structure **14** is derived from comparison with the more detailed analysis of the Zn^{II}–pyridylmonooxocyclam **16** (see later). Crystalline complex **14** as a monoperchlorate salt was isolated from pH 8 aqueous solution (see Experimental Section). Deprotonation of the amide group in complexation of peptide ligands often occurs with Cu^{II} and Ni^{II} ions, but rarely with the Zn^{II} ion.[28] Hence, this is an unusual case of amide N^-–Zn^{II} coordination, which undoubtedly is made possible due to the N_4 macrocyclic stabilization effects.[29] A similar structure of $[MH_{-1}L]^+$ was previously reported for complexes of **3** with Cu^{II} and Ni^{II}.[17]

From the analysis of the titration data at $I = 0.10$ ($NaClO_4$) and 25.0 ± 0.1 °C, the complex $[ZnH_{-1}L]^+$ (**14**) formation constant log $K(ZnH_{-1}L)$ (=log ($[[ZnH_{-1}L]^+]a_{H^+}/[Zn^{II}][L]$)) of 0.59 was determined (see Table I), which, as expected, is much smaller than those of 13.0 for Cu^{II} and 4.0 for Ni^{II}.[17] A postulated intermediate **12** should immediately transform to **14**, since **12** could not be detected by IR or NMR. A route to amide hydrolysis to **13** was not observed at all, indicating that the Zn^{II}-bound OH^- (if formed transiently) has no nucleophilic ability.

The titration curve for Cd^{II} with **3** (Figure 1b) implies weaker interaction (up to $a = 2$), and above pH 8, precipitation of $Cd^{II}(OH)_2$ occurs before the anticipated amide dissociation. These facts suggest incompatibility of a larger sized Cd^{II} ion with the square-planar monooxocyclam cavity size and/or insufficient acidity of Cd^{II} to displace the amide proton. A square planar Zn^{II} complex (trans III form) with cyclam (i.e. oxo-less macrocyclic tetraamine)[30] is more stable than a folded Cd^{II}–cyclam complex[31] (cis or trans I form): log $K(ZnL) = 15.5$[6a] vs log $K(CdL) = 11.7$.[31]

Pyridylmonooxocyclam Complexes with Zn^{II} and Cd^{II}. The 1:1 Zn^{II}– and Cd^{II}–$5\cdot4H^+$ titration curves are shown in parts c and b of Figure 2; both show inflections at $a = 2$ and 4. These titration curves at $2 < a < 4$ correspond to the loss of the four protons from the three secondary amines and the pyridyl N to form common $[ML]^{2+}$ complexes **15** and **17** (see Scheme II). Deprotonation of the amide group follows in the following steps ($4 < a < 5$) to produce $[MH_{-1}L]^+$ complexes **16** and **18**. The supporting evidence comes from the amide ν_{CO} changes in aqueous solutions from 1636 cm^{-1} for **15** ($[ZnL]^{2+}$, pD 6.5) to 1577 cm^{-1} for **16** ($[ZnH_{-1}L]^+$, pD 9) and 1611 cm^{-1} for **17** ($[CdL]^{2+}$, pD 8.5) to 1570 cm^{-1} for **18** ($[CdH_{-1}L]^+$, pD 12). In the first Cd^{II} complex **17**, the lower ν_{CO} of 1611 cm^{-1} is characteristic, which suggested an amide oxygen interaction with Cd^{II}, as indeed proved by the X-ray crystal analysis (see below). The amide oxygen coordination to Co^{III} similarly lowered ν_{CO} to 1625 cm^{-1}.[32]

From the analysis of the titration data at $a < 4$, the complex formation constants log $K(ML)$ (=log ($[[ML]^{2+}]/[M^{II}][L]$)) of 8.60 for **15** and 7.15 for **17** were determined at $I = 0.10$ ($NaClO_4$) and 25.0 ± 0.1 °C. The neutral four-nitrogen donors (three secondary N and pyridyl N) bind more strongly with Zn^{II} ion than with Cd^{II} ion. At $a > 4$, the amide deprotonation occurs with

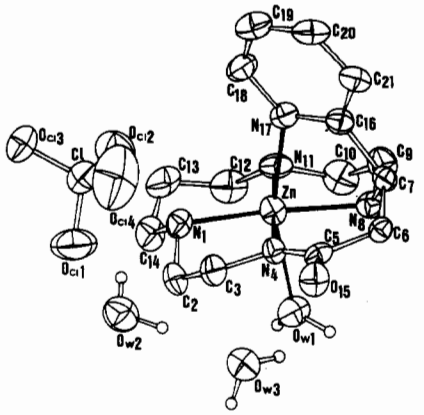

Figure 3. ORTEP drawing of $(16)ClO_4\cdot3H_2O$. Atoms are drawn with 30% probability ellipsoids.

Table II. Crystal Data and Data Collection Summary for the Salts of **16** and **17**

	$(16)ClO_4\cdot3H_2O$	$(17)(ClO_4)_2\cdot H_2O$
formula	$C_{15}H_{24}N_5OZnClO_4\cdot 3H_2O$	$C_{15}H_{25}N_5OCd(ClO_4)_2\cdot H_2O$
fw	509.3	620.7
cryst syst	triclinic	orthorhombic
space group	$P\bar{1}$	$P2_12_12_1$
cell dimens		
a, Å	10.075 (6)	11.512 (6)
b, Å	13.210 (6)	16.043 (9)
c, Å	8.937 (5)	12.471 (7)
α, deg	87.32 (4)	90
β, deg	109.01 (5)	90
γ, deg	101.09 (5)	90
V, Å^3	1103	2303
Z	2	4
d_{calcd}, g cm^{-3}	1.533	1.790
cryst color	colorless	colorless
radiation	Cu Kα (graphite monochromated)	
μ, cm^{-1}	31.4	105
2θ range, deg	6–130	6–156
scan speed, deg min^{-1}	6	6
no. of measd reflcns	3476	4766[a]
no. of reflcns for used refinement ($I > 2\sigma(I)$)	3476	2600
phasing	heavy atom method	
refinement	block-diagonal-matrix least-squares method	
final R	0.063	0.047
no. of refined atoms	30 (anisotropic) 30 H (isotropic)	33 (anisotropic) 25 H (isotropic)

[a] Of which 326 were symmetry equivalent (R_F between equivalent reflections was 0.075) and 1840 were Friedel pairs (R_F between Friedel pairs was 0.088).

(28) Freeman, H. C. *Adv. Protein Chem.* **1967**, *22*, 257–424.
(29) Thöm, V. J.; Fox, C. C.; Boeyens, J. C. A.; Hancock, R. D. *J. Am. Chem. Soc.* **1984**, *106*, 5947–5955.
(30) Kato, M.; Ito, T. *Inorg. Chem.* **1985**, *24*, 509–514.
(31) Thöm, V. J.; Hosken, G. D.; Hancock, R. D. *Inorg. Chem.* **1985**, *24*, 3378–3381.
(32) Collman, J. P.; Kimura, E. *J. Am. Chem. Soc.* **1967**, *89*, 6096–6103.

Table III. Final Fractional Coordinates ($\times 10^4$) for (**16**) $ClO_4 \cdot 3H_2O$ with Estimated Standard Deviations in Parentheses

atom	*x*	*y*	*z*	B_{eq}, Å^2
Zn	3012.4 (0.7)	2869.2 (0.5)	1124.1 (0.8)	2.86 (0.01)
N(1)	823 (4)	2865 (3)	186 (5)	3.0 (0.1)
C(2)	746 (5)	3818 (4)	−737 (6)	3.3 (0.1)
C(3)	1713 (5)	3917 (4)	−1767 (6)	3.3 (0.1)
N(4)	3110 (4)	3705 (3)	−814 (4)	2.7 (0.1)
C(5)	4181 (5)	3976 (3)	−1368 (5)	2.5 (0.1)
C(6)	5630 (5)	3697 (3)	−437 (6)	2.7 (0.1)
C(7)	5692 (5)	2780 (4)	687 (6)	2.8 (0.1)
N(8)	5244 (4)	3000 (3)	2049 (5)	2.8 (0.1)
C(9)	5513 (6)	2260 (4)	3359 (6)	3.9 (0.1)
C(10)	4435 (7)	2223 (5)	4235 (6)	4.2 (0.1)
N(11)	2981 (5)	1955 (3)	3098 (5)	3.4 (0.1)
C(12)	1832 (7)	2049 (4)	3773 (7)	4.1 (0.1)
C(13)	368 (7)	1896 (4)	2507 (8)	4.3 (0.1)
C(14)	66 (6)	2795 (5)	1373 (7)	3.9 (0.1)
O(15)	4136 (4)	4486 (3)	−2630 (4)	3.5 (0.1)
C(16)	4746 (5)	1822 (3)	−216 (6)	2.7 (0.1)
N(17)	3439 (4)	1530 (3)	−94 (5)	3.0 (0.1)
C(18)	2546 (6)	739 (4)	−1017 (7)	3.8 (0.1)
C(19)	2936 (7)	230 (4)	−2083 (7)	4.4 (0.1)
C(20)	4284 (7)	526 (4)	−2187 (7)	4.0 (0.1)
C(21)	5223 (6)	1319 (4)	−1230 (6)	3.5 (0.1)
O(W1)	3312 (4)	4345 (3)	2620 (4)	3.8 (0.1)
O(W2)	−880 (5)	3603 (3)	4449 (5)	4.8 (0.1)
O(W3)	1952 (4)	4767 (3)	4717 (4)	4.1 (0.1)
Cl	−1754 (1)	1103 (1)	6789 (2)	3.7 (0.0)
O(1Cl)	−2042 (7)	2082 (4)	7123 (7)	8.1 (0.1)
O(2Cl)	−1030 (6)	682 (4)	8246 (6)	7.6 (0.1)
O(3Cl)	−3088 (5)	450 (4)	6063 (6)	6.1 (0.1)
O(4Cl)	−942 (8)	1314 (7)	5787 (8)	11.2 (0.2)

Table IV. Bond Distances (Å) for (**16**)$ClO_4 \cdot 3H_2O$ and (**17**)$(ClO_4)_2 \cdot H_2O$, with Estimated Standard Deviations in Parentheses, and for the Ni^{II}–**5** complex[a]

16		**17**		Ni^{II}–**5** complex	
Zn–N(1)	2.088 (4)	Cd–N(1)	2.274 (7)	Ni–N(1)	2.065
Zn–N(4)	2.035 (4)	Cd–O(15)	2.509 (6)	Ni–N(4)	2.015
Zn–N(8)	2.120 (4)	Cd–N(8)	2.391 (6)	Ni–N(8)	2.065
Zn–N(11)	2.098 (4)	Cd–N(11)	2.300 (7)	Ni–N(11)	2.083
Zn–N(17)	2.266 (5)	Cd–N(17)	2.293 (7)	Ni–N(17)	2.142
Zn–O(W1)	2.354 (4)	Cd–O(W1)	2.356 (7)	Ni–O(W1)	2.166
N(1)–C(2)	1.467 (7)		1.477 (12)		1.485
N(1)–C(14)	1.490 (8)		1.496 (14)		1.491
C(2)–C(3)	1.537 (9)		1.512 (14)		1.526
C(3)–N(4)	1.435 (6)		1.466 (13)		1.472
N(4)–C(5)	1.338 (7)		1.333 (12)		1.305
C(5)–C(6)	1.499 (6)		1.510 (14)		1.524
C(6)–C(7)	1.530 (7)		1.540 (16)		1.545
C(7)–N(8)	1.489 (8)		1.471 (12)		1.478
N(8)–C(9)	1.463 (7)		1.502 (13)		1.484
C(9)–C(10)	1.528 (10)		1.498 (16)		1.518
C(10)–N(11)	1.504 (7)		1.479 (13)		1.480
N(11)–C(12)	1.487 (9)		1.484 (15)		1.485
C(12)–C(13)	1.539 (8)		1.491 (17)		1.522
C(13)–C(14)	1.512 (8)		1.550 (18)		1.531
C(16)–C(21)	1.378 (9)		1.403 (12)		1.380
C(18)–C(19)	1.368 (10)		1.384 (13)		1.372
C(19)–C(20)	1.406 (10)		1.353 (15)		1.362
C(20)–C(21)	1.443 (7)		1.383 (16)		1.394
C(7)–C(16)	1.586 (6)		1.513 (12)		1.519
C(5)–O(15)	1.277 (6)		1.250 (11)		1.282
C(16)–N(17)	1.372 (7)		1.335 (11)		1.339
N(17)–C(18)	1.411 (6)		1.377 (11)		1.339
Cl–O(1Cl)	1.420 (6)		1.435 (11)		1.404
Cl–O(2Cl)	1.390 (5)		1.403 (9)		1.355
Cl–O(3Cl)	1.491 (4)		1.409 (13)		1.283
Cl–O(4Cl)	1.399 (9)		1.393 (12)		1.342
Cl–O(1Cl2)			1.405 (11)		
Cl–O(2Cl2)			1.365 (9)		
Cl–O(3Cl2)			1.432 (10)		
Cl–O(4Cl2)			1.405 (13)		

[a] In this and the following tables, the data for the Ni^{II}–**5** complex are taken from ref. 20.

an estimated pK_a of 7.32 (for Zn^{II}) and 10.62 (for Cd^{II}) (see Scheme II). As shown by the lower pH buffer region, Zn^{II} yields a more stable amide-deprotonated complex (**16**) than Cd^{II} does (**18**). Their complex formation constants log $K(MH_{-1}L)$ (=log $([[MH_{-1}L]^+]a_{H^+}/[M^{II}][L])$) are 1.28 for Zn^{II} and −3.47 for Cd^{II} (see Table I). Taking advantage of these pH requirements for the amide deprotonation, one can easily distinguish the Zn^{II} ion from the Cd^{II} ion. Furthermore, a comparison of $K(ZnH_{-1}L)$ values for the 4-coordinate **14** (=0.59) and the 5-coordinate **16** (=1.28) indicates stability enhancement by the pendant pyridyl N coordination.

Table V. Bond Angles (deg) for (**16**)$ClO_4 \cdot 3H_2O$ and (**17**)$(ClO_4)_2 \cdot H_2O$, with Estimated Standard Deviations in Parentheses, and for the Ni^{II}–**5** Complex

	(**16**)$ClO_4 \cdot 3H_2O$ (M = Zn^{II})	(**17**)$(ClO_4)_2 \cdot H_2O$ (M = Cd^{II})	Ni^{II}–**5** complex
N(1)–M–N(11)	94.8 (2)	96.3 (3)	96.7
N(1)–M–O(W1)	94.7 (2)	89.5 (3)	90.8
N(8)–M–N(11)	88.3 (2)	77.5 (3)	85.1
N(8)–M–N(17)	81.0 (2)	71.5 (2)	79.1
N(17)–M–O(W1)	162.7 (1)	91.7 (3)	166.7
N(1)–M–N(4)	87.1 (2)		84.2
N(4)–M–N(8)	90.0 (2)		94.0
N(4)–M–N(17)	86.2 (2)		85.6
N(1)–M–O(15)		83.5 (2)	
O(15)–M–O(W1)		105.5 (3)	
O(15)–M–N(17)		75.2 (2)	
M–O(15)–C(5)		98.5 (5)	
M–N(17)–C(16)	102.8 (3)	115.4 (6)	109.9
N(1)–C(2)–C(3)	113.7 (4)	113.7 (8)	110.3
N(1)–C(14)–C(13)	114.9 (5)	113.8 (9)	112.5
C(2)–N(1)–C(14)	115.7 (4)	109.6 (7)	112.0
C(2)–C(3)–N(4)	109.3 (4)	114.0 (8)	109.3
C(3)–N(4)–C(5)	118.8 (4)	122.8 (8)	118.6
N(4)–C(5)–C(6)	119.4 (4)	116.7 (8)	119.1
C(5)–C(6)–C(7)	115.7 (4)	109.8 (8)	119.3
C(6)–C(7)–N(8)	112.1 (4)	109.1 (7)	109.9
C(7)–N(8)–C(9)	117.3 (4)	115.6 (7)	115.1
C(8)–C(9)–N(10)	113.0 (5)	109.0 (8)	109.1
C(9)–C(10)–N(11)	109.6 (5)	110.8 (6)	108.6
C(10)–N(11)–C(12)	113.9 (4)	112.3 (8)	114.3
N(11)–C(12)–C(13)	111.7 (5)	114.3 (10)	111.1
C(12)–C(13)–C(14)	112.0 (5)	114.5 (10)	115.2
N(4)–C(5)–O(15)	127.2 (4)	121.8 (8)	125.8
C(6)–C(5)–O(15)	113.3 (4)	121.1 (8)	115.2
C(6)–C(7)–C(16)	111.0 (4)	113.6 (8)	111.7
C(7)–C(16)—C(21)	118.3 (4)	120.1 (8)	121.5
N(8)–C(7)–C(16)	109.3 (4)	109.9 (7)	108.8
C(16)–C(21)–C(20)	117.9 (5)	118.7 (9)	118.5
C(18)–C(19)–C(20)	116.4 (6)	119.5 (9)	118.9
C(19)–C(20)–C(21)	122.7 (6)	120.4 (10)	119.3
C(7)–C(16)–N(17)	121.9 (4)	118.8 (8)	116.5
N(17)–C(18)–C(19)	121.7 (5)	120.9 (8)	122.7
C(16)–N(17)–C(18)	121.6 (4)	119.5 (7)	118.5

Table VI. Intermolecular Short Distances (Å) for (**16**)$ClO_4 \cdot 3H_2O$ and (**17**)$(ClO_4)_2 \cdot H_2O$ with Estimated Standard Deviations in Parentheses

(**16**)$ClO_4 \cdot 3H_2O$[a]		(**17**)$(ClO_4)_2 \cdot H_2O$[f]	
O(W3)···H′O(W1)	1.84 (10)	O(15)···HN(11)[g]	1.87 (10)
O(W3)···H′O(W2)	2.07 (9)	O(1Cl2)···HN(4)[h]	2.27 (10)
O(4Cl)···HO(W2)	2.27 (6)	O(3Cl2)···HN(8)[h]	2.27 (10)
O(15)···HO(W1)[b]	1.92 (6)	O(2Cl2)···HN(1)[i]	2.17 (10)
O(15)···H′O(W3)[c]	1.72 (6)		
O(3Cl)···HN(11)[d]	2.39 (6)		
O(W2)···HO(W3)[e]	1.78 (8)		

[a] Atoms marked with *b*, *c*, *d*, and *e* are at $(x, y, z - {}^1/_2)$, $(x, y, z - 1)$, $(x - {}^1/_2, y - {}^1/_2, z)$, and $(x - {}^1/_2, y, z)$, respectively. [f] Atoms marked with *g*, *h*, and *i* are at $(-{}^1/_2 - x, -y, -{}^1/_2 + z)$, $(-{}^1/_2 + x, {}^1/_2 - y, -z)$, and $(-{}^1/_2 - x, -y, -{}^1/_2 + z)$, respectively.

X-ray Crystal Structure of $[ZnH_{-1}L]^+$ (16). Figure 3 shows an ORTEP drawing of (**16**)$ClO_4 \cdot 3H_2O$ with 30% probability thermal ellipsoids. Crystal data and data collection parameters are displayed in Table II. The atomic positional parameters are given in Table III. Selected interatomic distances and bond angles are listed in Tables IV and V. Short hydrogen-bond distances are presented in Table VI.

Table VII. Final Fractional Coordinates ($\times 10^4$) for $(17)(ClO_4)_2 \cdot H_2O$ with Estimated Standard Deviations in Parentheses

atom	x	y	z	B_{eq}, Å^2
Cd	−1737.0 (0.4)	315.3 (0.3)	−1070.1 (0.4)	2.38 (0.01)
N(1)	88 (6)	565 (4)	−1690 (6)	3.1 (0.1)
C(2)	381 (9)	1323 (7)	−2304 (8)	4.1 (0.1)
C(3)	−285 (9)	1407 (6)	−3344 (7)	4.1 (0.1)
N(4)	−1471 (7)	1723 (5)	−3211 (6)	3.5 (0.1)
C(5)	−2382 (8)	1226 (6)	−3050 (7)	3.3 (0.1)
C(6)	−3523 (8)	1645 (7)	−2793 (9)	4.4 (0.2)
C(7)	−3851 (7)	1480 (5)	−1614 (9)	3.5 (0.1)
N(8)	−2813 (6)	1586 (4)	−939 (6)	3.0 (0.1)
C(9)	−3033 (9)	1635 (6)	246 (8)	4.2 (0.1)
C(10)	−1900 (11)	1559 (6)	827 (7)	4.6 (0.2)
N(11)	−1389 (7)	722 (5)	669 (6)	3.6 (0.1)
C(12)	−149 (11)	688 (8)	991 (8)	5.4 (0.2)
C(13)	669 (11)	1043 (9)	186 (10)	5.8 (0.2)
C(14)	925 (8)	464 (7)	−781 (11)	5.6 (0.2)
O(15)	−2279 (6)	451 (4)	−3011 (5)	3.9 (0.1)
C(16)	−4375 (7)	628 (6)	−1427 (7)	3.1 (0.1)
N(17)	−3680 (6)	3 (4)	−1129 (6)	3.0 (0.1)
C(18)	−4143 (8)	−778 (6)	−970 (8)	3.6 (0.1)
C(19)	−5321 (8)	−920 (6)	−1094 (8)	4.1 (0.1)
C(20)	−6022 (8)	−287 (8)	−1400 (9)	4.9 (0.2)
C(21)	−5570 (8)	501 (7)	−1574 (9)	4.3 (0.1)
O(W)	−1244 (7)	−1098 (4)	−826 (11)	7.6 (0.2)
Cl(1)	−1796 (2)	3103 (1)	4243 (2)	3.8 (0.0)
O(1Cl1)	−2706 (9)	2631 (7)	4743 (10)	7.9 (0.2)
O(2Cl1)	−2084 (11)	3941 (5)	4065 (11)	9.9 (0.2)
O(3Cl1)	−1601 (18)	2728 (8)	3237 (10)	12.7 (0.4)
O(4Cl1)	−780 (9)	3009 (9)	4837 (11)	10.7 (0.3)
Cl(2)	−6127 (2)	1334 (1)	1644 (2)	3.9 (0.0)
O(1Cl2)	−7145 (9)	1543 (7)	2206 (10)	8.4 (0.2)
O(2Cl2)	−6097 (16)	511 (5)	1371 (11)	12.2 (0.3)
O(3Cl2)	−6039 (10)	1867 (6)	726 (8)	7.4 (0.2)
O(4Cl2)	−5169 (11)	1522 (8)	2299 (11)	10.3 (0.3)

The square-planar N_4 coordination with Zn^{II} is evident with the monooxocyclam moiety composed of three NH's and a deprotonated amide N^-. These four donor atoms, N(1), N(8), N(11), and N(4), are nearly coplanar. The macrocycle conformation is similar to a chair form adopted by the most stable cyclam complex.[29] As anticipated, the Zn–amide N(4) bond distance is shorter at 2.035 (4) Å than other Zn^{II}–NH distances (average 2.10 Å). The present square-planar macrocyclic structure should be roughly the same as that of the previous $[ZnH_{-1}L]^+$ complex **14**, since both show a similar amide ν_{CO}. The pyridine ring stands vertically above the N_4 plane to allow its nitrogen donor N(17) to give the fifth coordination point from an apical site (2.266 Å) but its apical bonding is appreciably tilted (N(17)–Zn–N(4) = 86.2°, N(17)–Zn–N(8) = 81.0°) from perpendicular. At the other apical site is a weakly bound H_2O (2.354 Å).

Earlier, we reported an X-ray crystal structure of a high spin Ni^{II} complex with **5**,[20] which had an identical formula $[NiH_{-1}L]^+$ with a similar square-pyramidal N_5 structure (with an identical macrocyclic configuration). For the sake of comparison, we list the corresponding bond parameters for the Ni^{II} complex in Tables IV and V. The equatorial Ni^{II}–NH (average 2.07 Å) and Ni^{II}–N^- (2.015 Å) bonds are a little shorter. The apical N(17)–Ni^{II}–O(W1) bond is more straight (166.7°) than that (162.7°) of the Zn^{II} complex **16**, and the N(17)–Ni^{II} distance of 2.14 Å is much shorter. The sixth site apical bond to H_2O is also shorter; Ni^{II}–O(W1) = 2.17 Å. These and other differences in bond parameters between the high-spin Ni^{II} and the Zn^{II} complexes may reflect the difference in their ligand field strengths: Ni^{II} (d^8) would force a more strict octahedral structure to cause some strain on the ligand side, while with Zn^{II} (d^{10}) the ligand would be subject to a less deformed conformation.

X-ray Crystal Structure of $[CdL]^{2+}$ (17). Figure 4 shows an ORTEP drawing of $(17)(ClO_4)_2 \cdot H_2O$ with 30% probability thermal ellipsoids. Crystal data and data collection parameters are displayed in Table II. The atomic positional parameters are given in Table VII. Selected interatomic distances and bond angles are listed in Tables IV and V. Short hydrogen-bond distances are presented in Table VI.

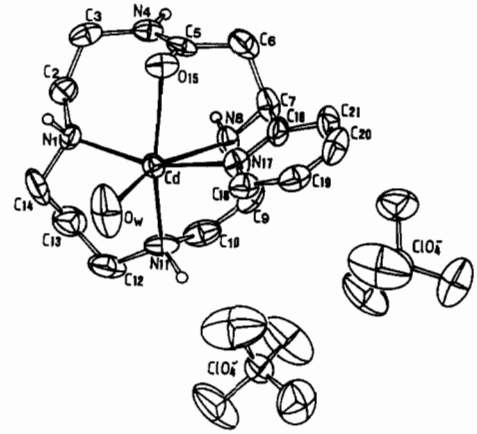

Figure 4. ORTEP drawing of $17(ClO_4)_2 \cdot H_2O$. Atoms are drawn with 30% probability ellipsoids.

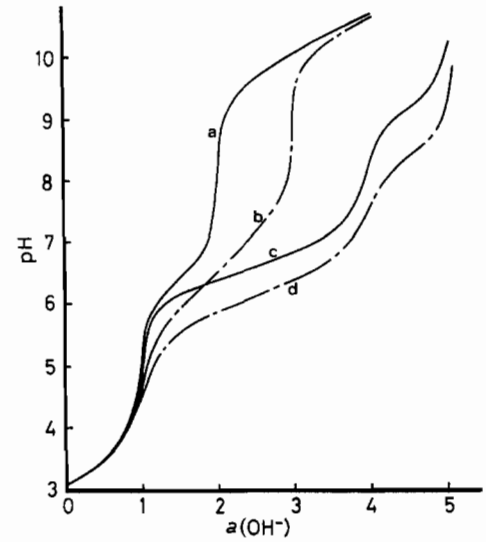

Figure 5. Titration curves for (hydroxyphenyl)oxocyclam **6** and (1-hydroxy-4-nitrophenyl)monooxocyclam **8**: (a) 1 mM of $[6 \cdot 3H^+]^{3+}$; (b) 1 mM of $[8 \cdot 3H^+]^{3+}$; (c) solution a + 1 mM of $ZnSO_4$; (d) solution b + 1 mM of $ZnSO_4$.

Scheme III

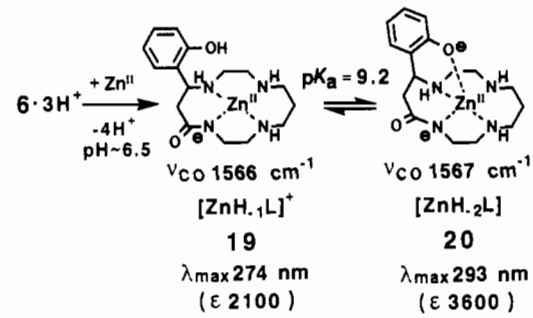

The folded, cis coordination is evident in the monooxocyclam part with three NH's and an amide oxygen. The Cd^{II} ion lies in a distorted octahedral environment with two more donors, the pendant pyridine and a water molecule. The Cd^{II}–O(amide) bonding is evident, although its distance of 2.509 (6) Å is longer than the average (2.31 Å) for Cd^{II}–amine bonding. The amide oxygen bond to Cd^{II} causes some strain in the cyclam conformation with an angle of 98.5° for Cd^{II}–O(15)–C(5). The larger size of Cd^{II} than Zn^{II} and additional coordination of pyridyl N make such a rare macrocyclic coordination possible.

(Hydroxyphenyl)monooxocyclam (6) Complex with Zn^{II}. (Hydroxyphenyl)-(**6**) and (1-hydroxy-4-nitrophenyl)monooxocyclams (**8**)[21,22] have phenolic hydrogens at positions close enough to compete with the amide hydrogen for Zn^{II} ions. An immediate question is which of the dissociable hydrogens (pK_a of ca. 10 (**6**)

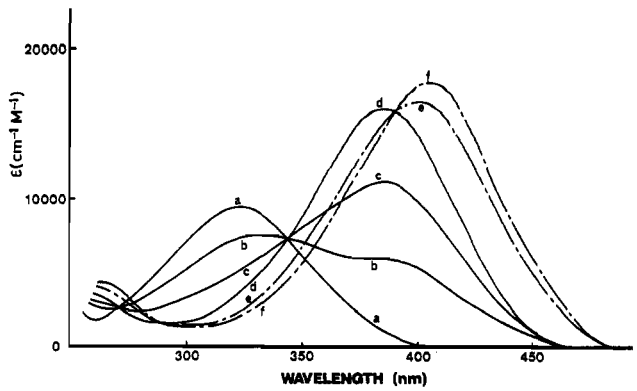

Figure 6. UV absorption spectra (λ_{max} (ϵ)) for (1-hydroxy-4-nitrophenyl)monooxocyclam **8** at 25 °C and I = 0.1 M ($NaClO_4$): (a) [**8**·$2H^+]^{2+}$, 319 nm (9000), pH 4.3; (b) pH 5.7; (c) pH 6.1; (d) **22**, 385 nm (15 300), pH 7.5; (e) pH 8.8; (f) **23**, 405 nm (17 200), pH 9.8.

and ca. 7 (**8**) for phenolic hydrogen or pK_a of ca. 16 for amide[33] hydrogen) is removed first in complexation with Zn^{III} ion.

The 1:1 Zn^{II}–**6**·$3H^+$ titration curve shows inflections at a = 1 and 4 (Figure 5c). The buffer region at $1 < a < 4$ was assigned to the loss of four protons including an amide deprotonation to the complex $[ZnH_{-1}L]^+$ (**19**) which was similar to **14** (see Scheme III). The following step ($4 < a < 5$) involves deprotonation of the phenol to $[ZnH_{-2}L]^+$ (**20**). This deprotonation sequence is concluded from the following evidences: (i) The amide CO stretching frequency lowers from 1632 cm^{-1} for **6** to 1566 cm^{-1} for **19** (pD 8), which remains the same (1567 cm^{-1}) for **20** (pD 12). (ii) The UV absorption maximum of the pendant phenol in **19** (274 nm, ϵ = 2100, at pH 7.5) indicates the undissociated form, which shifts to longer wavelength (293 nm, ϵ = 3600) at pH 11 in agreement with the phenolate anion form **20**. Hence, in complexation of **6** with Zn^{II} ion, the amide proton (ordinarily less acidic) is more prone to dissociate than the phenolic proton (more acidic). This is obviously due to the great advantage of N^- formation for the macrocyclic N_4 coordination.

It is of interest to compare the pendant phenolate UV absorptions for the monooxocyclam (N_3N^-) system **20** and the cyclam (N_4) system **21**, the latter having been characterized by an

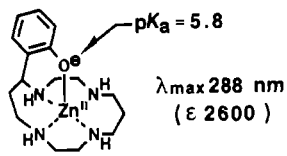

21

X-ray crystal analysis.[34] The UV maximum differs from 293 nm for **20** to 288 nm for **21**. The corresponding Zn^{II}-unbound phenolate anions show λ_{max} = 293 nm (ϵ = 4000) and 292 nm (ϵ = 4000),[22] respectively. Taken together, the phenolate–Zn^{II} bonding in the present complex **20** is considered weaker and more ionic in nature than the corresponding bonding in the cyclam complex **21**. This conclusion is also supported by the phenol pK_a value of 9.2 for **20** against the unusually lowered value of 5.8 for **21**. We ascribe such a weak Zn^{II}–phenolate anion interaction in **20** to a weakened acidity of Zn^{II} already bound with an amide anion. Yet, the pK_a value of 9.2 for **19** is lower by 0.4 log unit than that for the free ligand **6**, indicating the weak interaction between the phenolate and the Zn^{II} ion (or the apical coordinated water).

(1-Hydroxy-4-nitrophenyl)monooxocyclam (8) Complex with Zn^{II}. When the acidity of the pendant phenol is increased from pK_a 9.6 to 7.2 by the 4-nitro group, the sequence of the anion coordination becomes reversed. Although the titration curve for

Scheme IV

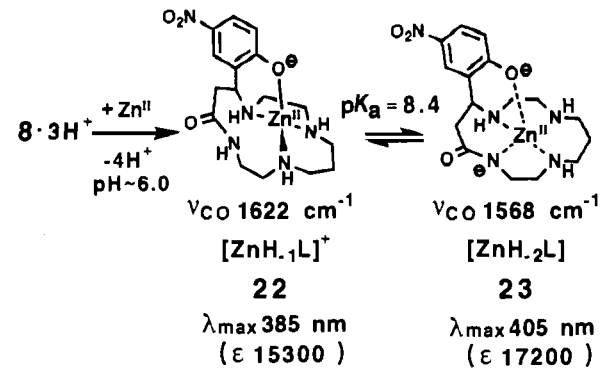

(1-hydroxy-4-nitrophenyl)monooxocyclam **8** (Figure 5d) is similar to the one for the (hydroxyphenyl)monooxocyclam **6** (Figure 5c), the 1-hydroxy-4-nitrophenyl dissociation occurs in the buffer region at $1 < a < 4$ to give **22**. The UV absorption maximum of the undissociated 1-hydroxy-4-nitrophenyl group in **8** (322 nm, ϵ = 9000, at pH 4.3) shifts at pH 7.5 to longer wavelength indicating formation of the phenolate complex $[ZnH_{-1}L]^+$ (**22**) (385 nm, ϵ = 15 300) with two isosbestic points due to the equilibrium between **8** and **22** (see Figure 6a–d). In the second buffer region at $4 < a < 5$, the loss of the amide proton proceeds to $[ZnH_{-2}L]$ (**23**) (see Scheme IV). The amide CO stretching frequency changed from 1630 cm^{-1} for 8 and 1622 cm^{-1} for **22** (pD 7.5) to 1568 cm^{-1} for **23** (pD 11).

In the second deprotonation process from **22** to **23**, the UV absorption peak shifts further to longer wavelength (λ_{max} = 405 nm, ϵ = 17 200, at pH 9.8) (see Figure 6d–f). This is interpreted to mean that the equatorial amide anion coordination makes the phenolate–Zn^{II} bonding more ionic (weaker) in **23** from a more covalent (stronger) bonding type in **22**. The UV absorption of **23** (Figure 6f) is nearer to that of the uncoordinating phenolate anion of free ligand **8** at pH 11 (λ_{max} = 409 nm, ϵ = 17 000). In the absence of other anion binding as demonstrated by the (1-hydroxy-4-nitrophenyl)cyclam[22] complex **24**, the Zn^{II}–phenolate

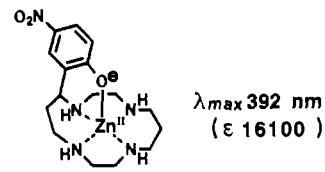

24

bonding becomes stronger than that for **23**, as evidenced by λ_{max} = 392 nm (ϵ = 16 100). These differences in the UV absorption of the 1-hydroxy-4-nitrophenylate moiety suggest that the nonionic N_3-coordinated Zn^{II} ion (in **22**) is a stronger acid than that in the N_4 (in **24**) and N_3N^- (in **23**) systems.

From the analysis of the titration data of Figure 5c,d, the complex formation constants log $K(ZnH_{-1}L)$ of −0.4 for **19** and of −1.7 for **22** were determined, indicating that the macrocyclic N_3N^- structure **19** is more stable than the 4-coordinate (possibly tetrahedral) N_3O^- structure **22**. The deprotonation constants (pK_a) of 9.2 and 8.4 (at $4 < a < 5$) are obtained for the phenol dissociation of the (hydroxyphenyl)monooxocyclam complex **19** (Figure 5c) and the amide dissociation of the (1-hydroxy-4-nitrophenyl)monooxocyclam complex **22** (Figure 5d), respectively (see Schemes III and IV). The final complex formation constants log $K(ZnH_{-2}L)$ of −9.6 for **20** and of −10.1 for **23** were calculated from the pK_a values and the $K(ZnH_{-1}L)$ values (see Table I).

Unlike Zn^{II}, the Cd^{II} ion has negligible interaction with **6** and **8** and the complexation analysis cannot be made.

Recently, we introduced a hydroxyphenyl[12]aneN_3 Zn^{II} complex, **25**, as a simplified anion inhibition model of carbonic anhydrase.[12] This phenol dissociates with a pK_a value as low as 6.8 to complete 4-coordination.[11] The ionization constant of Zn^{II}–OH_2 in **25** is reduced to pK_a = 10.7 from pK_a = 7.3 of **1**. The present data with Zn^{II}–**6** and –**8** also illustrate that the two

(33) Pine, S. H.; Hendrickson, J. B.; Cram, D. J.; Hammond, G. S. *Organic Chemistry*, 3rd Japanese ed.; Hirokawa: Tokyo, 1980.
(34) Kimura, E.; Koike, T.; Toriumi, K. Unpublished data (the Zn^{II}–O^- (phenolate) bond length of **21** is 1.98 Å).

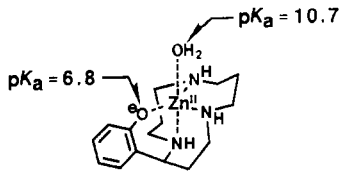

25

intramolecular anions mutually weaken the acidity of the Zn^{II} ion. In other words, the Zn^{II} ion does not welcome simultaneous coordination of two anions.

Previously, we reported the dioxocyclam system **4**,[13,20] which with Cu^{II} or Ni^{II} forms square-planar $[MH_{-2}L]$ complexes, containing the two deprotonated amide N^-–M^{II} bonds. Therefore, we studied pH titration of Zn^{II} and Cd^{II} with **4** and found no interaction with Zn^{II} and Cd^{II} ions. This fact supports the insufficient acidity of Zn^{II} and Cd^{II} to simultaneously accommodate the *two* amide anions.

Monooxo[16]aneN$_5$ (10) Complexes with Zn^{II} and Cd^{II}. Finally, a larger sized macrocyclic ligand, **10**,[18] containing five potential N donors in a ring was tested. The 1:1 Zn^{II}– and Cd^{II}–**10**·$4H^+$ titration curves are shown in parts b and c of Figure 7, which show inflections at $a = 1$ and 4. The titration curves at $a < 4$ were assigned to the loss of four protons from H_2N^+'s to give a common formulation of $[ML]^{2+}$ complexes, **26** and **28** (see Scheme V). In the next step at $4 < a < 5$, the amide group deprotonates to form $[MH_{-1}L]^+$ complexes **27** and **29**. The supporting evidence is the amide ν_{CO} changes (in D_2O) from 1637 cm^{-1} for **26** ($[ZnL]^{2+}$, pD 7) to 1559 cm^{-1} for **27** ($[ZnH_{-1}L]^+$, pD 9.5) and 1637 cm^{-1} for **28** ($[CdL]^{2+}$, pD 8) to 1560 cm^{-1} for **29** ($[CdH_{-1}L]^+$, pD 12).

From the analysis of the titration data for $1 < a < 4$, the Zn^{II} complex **26** and Cd^{II} complex **28** formation constants log K(ML) of 10.7 and 11.6, respectively, were determined. As immediately shown by the lower buffer region (at $1 < a < 4$) for Cd^{II} than that for Zn^{II}, the larger sized Cd^{II} ion binds more strongly than the smaller sized Zn^{II} ion with the fairly loose N_4 macrocycle. At higher pH, however, Zn^{II} yields a *more stable* deprotonated amide coordinated complex, **27**, than Cd^{II} does, **29**, as clearly demonstrated by the reversed pH buffer regions at $4 < a < 5$. The amide deprotonation constants (pK_a) are 8.4 (for Zn^{II}) and 10.5 (for Cd^{II}) (see Scheme V). The final complex formation constants log $K(MH_{-1}L)$ of 2.3 for Zn^{II} and 1.1 for Cd^{II} are calculated from the pK_a values and the K(ML) values (see Table I). The pK_a value of 8.4 for the amide deprotonation of the Zn^{II}-complex **26** is one order higher than that of **15** (see Table I). It probably is due to the fact that the smaller sized Zn^{II} ion would prefer the smaller 14-membered macrocycle to the larger 16-membered one. By contrast, with the larger sized Cd^{II} ion the pK_a values (10.5 and 10.6) are insensitive to these ligand types.

The most significant finding for the large-sized macrocycle ***10*** *is that the Zn^{II} and Cd^{II} complex stability orders reverse on passage to the amide deprotonation.* This novel fact vividly tells us about the difference of the coordination properties between Zn^{II} and Cd^{II} ions. This significance may be more emphasized in the light of the fact that the oxo-less 16-membered pentaamine ligand yields a more stable Cd^{II} complex (log K(CdL) = 18.1) than a Zn^{II} complex (log K(ZnL) = 17.9).[6a] It is also remarkable that here the pK_a values for the amide deprotonation with Zn^{II} and Cd^{II} differ by 2–3 orders of magnitude. In the Cd^{II}-substituted carbonic anhydrase, the pK_a value for the Cd^{II}–OH_2 moiety is estimated to be higher by an order of 2–3 (i.e. $pK_a \simeq 9$).[35,36]

Concluding Remarks

The acidity of Zn^{II} toward H_2O is an essential feature of many Zn^{II} enzymes. The present study has disclosed that a series of dissociable hydrogen-containing macrocyclic polyamines **3**–**10** are

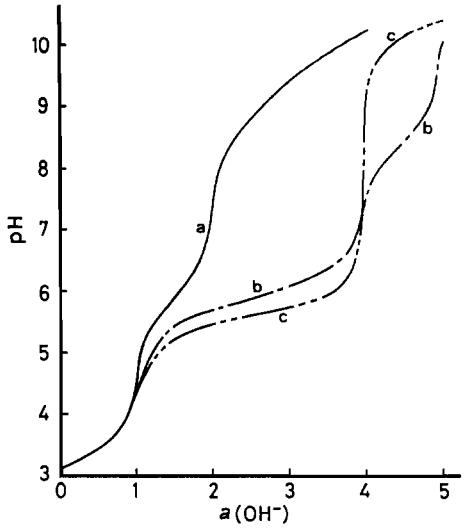

Figure 7. Titration curves for monooxo[16]aneN$_5$ **10**: (a) 1 mM of $[$**10**·$4H^+]^{4+}$; (b) solution a + 1 mM of $ZnSO_4$; (c) solution a + 1 mM of $CdSO_4$.

Scheme V

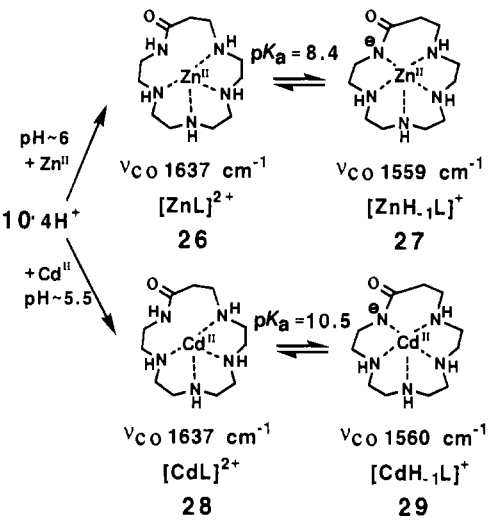

an appropriate system to distinguish Zn^{II} from Cd^{II} in their inherent acid properties. The results show the following. (i) The pK_a value of the secondary amide (normally ca. 16)[33] drastically varies according to the proximate Zn^{II} environments. The pK_a value of water (15.7), which incidentally is almost the same as that of the amide, should also be influenced by the nearby Zn^{II}. Thus, the variation of the amide pK_a values would be parallel to the variation of the water pK_a values. It is discovered here that the Zn^{II} acidity (as measured toward amides) is stronger in the smaller sized macrocycle (e.g. **3**) than in the larger sized **10**. (ii) Between Zn^{II} and Cd^{II}, the acidity of Zn^{II} is more significantly affected by the macrocyclic ligand size and the additional donor than is the acidity of Cd^{II}. A larger sized Cd^{II} ion is generally less sensitive to the ligand size and is less acidic than the Zn^{II} ion by ca. 2–3 orders of magnitude. (iii) The monooxocyclam **3** can separate Zn^{II} from Cd^{II} by its selective sequestering ability for Zn^{II}. (iv) Attachment of one anion (1-hydroxy-4-nitrophenylate) already reduces the Zn^{II} acidity toward the second (amide) deprotonation (from 7.3 for the pyridyl-pendant system **5** to 8.4 for the 1-hydroxy-4-nitrophenylate-pendant system **8**). This is also true with the acidity of Zn^{II}–OH_2 (apical) in the N_3N^- complex **14** ($pK_a > 12$) and in the N_4 cyclam complex ($pK_a = 9.8$).[34] (v) These observations may be extendable to explain the anion inhibition effect as seen in carbonic anhydrase,[37] which would reduce

(35) Coleman, J. E.; Gettins, P. In ref 1. Chapter 6.
(36) Recently, **10** has been shown to complex also with the Hg^{II} ion (log K(HgL) = 22.8 and log $K(HgH_{-1}L)$ = 14.1: Kodama, M.; Kimura, E. *Bull. Chem. Soc. Jpn.* **1989**, *62*, 3093–3097).
(37) Pocker, Y.; Deits, T. L. *J. Am. Chem. Soc.* **1982**, *104*, 2424–2434. Yachandra, V.; Powers, L.; Spiro, T. G. *J. Am. Chem. Soc.* **1983**, *105*, 6596–6604.

the acidity of Zn^{II}. (vi) In carboxypeptidase A, Zn^{II} is coordinated with two N (from two histidines, His(69), His(196)) and one anionic O^- (from the carboxylate of Glu(72)).[38] These ligands would not make the Zn^{II} ion acidic enough to produce a Zn^{II}–OH^- species from Zn^{II}–OH_2. Only with the cooperation of COO^- (Glu(270)) can the Zn^{II}-bound water come to act as a reactive nucleophile.[39] Our present experimental data for this model are compatible with this interpretation. In the recent ab initio calculation, Bertini et al. found a similar acidity-weakening effect by anionic ligands ($HCOO^-$ and CH_3S^-).[40] (vii) Finally, in actual Zn^{II} enzymes, there might be special environmental devices for the Zn^{II}–OH^- moiety to work as a nucleophile. Otherwise, Zn^{II}–OH^- might merely act as a base to dissociate a proton from the nearby peptides.

(38) Rees, D. C.; Lewis, M.; Honzatko, R. B.; Lipscomb, W. N.; Hardman, K. D. *Proc. Natl. Acad. Sci U.S.A.* **1981**, *78*, 3408–3412.
(39) Christianson, D. W.; Lipscomb, W. N. *Acc. Chem. Res.* **1989**, *22*, 62.
(40) Bertini, I.; Luchinat, C.; Rosi, M.; Sgamellotti, A.; Tarantelli, F. *Inorg. Chem.* **1990**, *29*, 1460.

Registry No. **3**, 85828-26-8; **5**, 108643-56-7; **6**, 129620-89-9; **8**, 129620-90-2; **10**, 91328-02-8; (**14**)ClO_4·$2H_2O$, 129648-16-4; (**15**)$(ClO_4)_2$·$2H_2O$, 129648-18-6; (**16**)ClO_4·H_2O, 129620-92-4; (**16**)ClO_4·$3H_2O$, 129648-19-7; (**17**)$(ClO_4)_2$·H_2O, 129620-94-6; (**18**)ClO_4·H_2O, 129620-96-8; (**19**)ClO_4·$2H_2O$, 129620-98-0; (**20**)·H_2O, 129620-99-1; (**22**)ClO_4·$2H_2O$, 129621-01-8; (**23**)·H_2O, 129621-02-9; (**26**)$(ClO_4)_2$·$2H_2O$, 129621-04-1; (**27**)ClO_4·H_2O, 129621-06-3; (**28**)$(ClO_4)_2$·$2H_2O$, 129621-08-5; (**29**)ClO_4·H_2O, 129621-10-9.

Supplementary Material Available: Tables listing thermal parameters and the derived hydrogen positions for **16** and **17** (4 pages); tables of calculated and observed structure factors for **16** and **17** (13 pages). Ordering information is given on any current masthead page.

Contribution from the Departments of Chemistry, University of Minnesota, Minneapolis, Minnesota 55455, and University of New Orleans, New Orleans, Louisiana 70122

Structures and Properties of Dibridged (μ-Oxo)diiron(III) Complexes. Effects of the Fe–O–Fe Angle

Richard E. Norman,[†] Richard C. Holz,[†] Stéphane Ménage,[†] Charles J. O'Connor,[‡] Jian H. Zhang,[‡] and Lawrence Que, Jr.*[,†]

Received May 14, 1990

A series of (μ-oxo)diiron(III) complexes of tris(2-pyridylmethyl)amine (TPA), $[Fe_2(TPA)_2O(L)](ClO_4)_n$, were synthesized and characterized where L represents the bridging ligands carbonate, hydrogen maleate, diphenyl phosphate, diphenylphosphinate, maleate, and phthalate. Together with the linear dichloride complex, this series of compounds provides a unique opportunity to systematically study the effects of the Fe–O–Fe angle (125–180°) on the electronic spectral and magnetic properties of the (μ-oxo)diiron(III) core. $[Fe_2(TPA)_2O(CO_3)](ClO_4)_2$·$2CH_3OH$ (**1**) crystallizes in the monoclinic space group $P2_1/c$ with a = 11.282 (7) Å, b = 18.253 (9) Å, c = 20.390 (7) Å, and β = 95.02 (4)°. The structure was determined at −50 °C from 4544 out of a total of 8154 reflections with R = 0.068 and R_w = 0.080. $[Fe_2(TPA)_2O(maleateH)](ClO_4)_3$·$2CH_3COCH_3$ (**4**) crystallizes in the monoclinic space group $P2_1/n$ with a = 21.604 (6) Å, b = 11.76 (1) Å, c = 22.150 (7) Å, and β = 115.62 (3)°. The structure was determined at −50 °C from 4832 out of a total of 7043 reflections with R = 0.072 and R_w = 0.089. $[Fe_2(TPA)_2O(phthalate)](ClO_4)_2$·$CH_3OH$·$H_2O$ (**9**) crystallizes in the monoclinic space group $P\bar{1}$ with a = 12.170 (5) Å, b = 12.982 (9) Å, c = 17.070 (7) Å, α = 77.26 (7)°, β = 115.62 (3)°, and γ = 62.76 (6)°. The structure was determined at −32 °C from 3592 out of a total of 8329 reflections with R = 0.059 and R_w = 0.069. X-ray crystallographic studies of **1**, **4**, and **9** establish the presence of a doubly bridged diiron core in which complexes **1** and **4** contain distinct iron centers bridged by μ-1,3-carboxylates while **9** exhibits a symmetric diiron core bridged by a μ-1,6-phthalate. These studies also reveal that the (μ-oxo)diiron(III) core expands on going from **1** to **4** to **9** due to the increasing bites of the bridging ligands. The Fe–O–Fe bond angles of **1**, **4**, and **9** are 125.4, 131.0, and 143.4°, respectively, while the Fe···Fe distances are 3.196, 3.261, and 3.402 Å, respectively. ^1H NMR spectra indicate that the iron(III) centers of **1** and **4** remain distinct in solution while **9** retains its symmetric structure. While the magnetic properties of the complexes appear to be independent of the Fe–O–Fe angle, the visible absorption features of the complexes systematically blue shift as the Fe–O–Fe angle increases. The latter trend suggests that the visible bands are dominated by oxo-to-Fe(III) charge-transfer transitions.

Introduction

The (μ-oxo)diiron(III) unit has been the subject of considerable interest among inorganic chemists for several years.[1-3] This interest has further intensified[4] due to the discovery of a (μ-oxo)bis(μ-carboxylato)diiron(III) core in methemerythrin[5] and an analogous (μ-oxo)(μ-carboxylato)diiron(III) core in *Escherichia coli* ribonucleotide reductase.[6] The electronic spectra of methemerythrin[7,8] and ribonucleotide reductase[9] are rich with absorption features stretching from the UV region to the near-IR region. On the basis of a study of $[Fe_2O(HEDTA)_2]^{2-}$,[10] these features were initially proposed[11] to arise from simultaneous pair excitations of ligand field transitions, the forbiddenness of these transitions being partially lifted by the presence of antiferromagnetic coupling between the iron centers. However, more recent studies[7] on hemerythrin, employing a combination of polarized

(1) (a) Murray, K. S. *Coord. Chem. Rev.* **1974**, *12*, 1–35. (b) Kurtz, D. M., Jr. *Chem. Rev.* **1990**, *90*, 585–606.
(2) Ercolani, C.; Gardini, M.; Murray, K. S.; Pennesi, G.; Rossi, G. *Inorg. Chem.* **1986**, *25*, 3972–3976.
(3) Mukherjee, R. N.; Stack, T. D. P.; Holm, R. H. *J. Am. Chem. Soc.* **1988**, *110*, 1850–1861.
(4) (a) Que, L., Jr.; True, A. E. *Prog. Inorg. Chem.*, in press. (b) Sanders-Loehr, J. In *Iron Carriers and Iron Proteins*, Loehr, T. M., Ed.; VCH: New York, 1989; pp 373–466. (c) Que, L., Jr.; Scarrow, R. C. *ACS Symp. Ser.* **1988**, *372*, 152–178. (d) Lippard, S. J. *Angew. Chem., Intl. Ed. Engl.* **1988**, *27*, 344–361.
(5) (a) Stenkamp, R. E.; Sieker, L. C.; Jensen, L. H. *J. Am. Chem. Soc.* **1984**, *106*, 618–622. (b) Klotz, I. M.; Kurtz, D. M., Jr. *Acc. Chem. Res.* **1984**, *17*, 16–22.
(6) (a) Nordlund, P.; Sjöberg, B.-M.; Eklund, H. *Nature* **1990**, *345*, 593–598. (b) Reichard, P.; Ehrenberg, A. *Science (Washington, D.C.)* **1983**, *221*, 514–519. (c) Lynch, J. B.; Juarez-Garcia, C.; Münck, E.; Que, L., Jr. *J. Biol. Chem.* **1989**, *264*, 8091–8096.
(7) Reem, R. C.; McCormick, J. M.; Richardson, D. E.; Devlin, F. J.; Stephens, P. J.; Musselman, R. L.; Solomon, E. I. *J. Am. Chem. Soc.* **1989**, *111*, 4688–4704.
(8) Sanders-Loehr, J.; Loehr, T. M.; Mauk, A. G.; Gray, H. B. *J. Am. Chem. Soc.* **1980**, *102*, 6992–6996.
(9) Petersson, L.; Gräslund, A.; Ehrenberg, A.; Sjöberg, B.-M.; Reichard, P. *J. Biol. Chem.* **1980**, *255*, 6706–6712.
(10) The following abbreviations are used throughout: HEDTA, *N*-(hydroxyethyl)ethylenediamine-*N*,*N*′,*N*′-triacetic acid; HDP, *N*-(2-hydroxybenzyl)-*N*,*N*-bis(2-pyridylmethyl)amine; TPA, tris(2-pyridylmethyl)amine; Me_3tacn, 1,4,7-trimethyl-1,4,7-triazacyclononane; HB($pz)_3$, hydrotris(pyrazolyl)borate; BPA, bis(2-pyridylmethyl)amine; BBA, bis(2-benzimidazolylmethyl)amine; tpbn, *N*,*N*,*N*′,*N*′-tetrakis(2-pyridylmethyl)-1,4-diaminobutane.
(11) Schugar, H. J.; Rossman, G. R.; Barraclough, C. G.; Gray, H. B. *J. Am. Chem. Soc.* **1972**, *94*, 2683–2690.

0020-1669/90/1329-4629$02.50/0